A Hard-Sphere Model to Simulate Alloy Thin Films

Abstract: A model is developed for the simulation of alloy thin films by forming a layer consisting of spheres of two different sizes mixed randomly in any desired proportion. Included in the model is the possibility for vibration to simulate low-temperature annealing, as well as the use of a "substrate" containing periodic grooves to simulate epitaxial growth. Optical (Fraunhofer) diffraction patterns are taken from photographs of the model for comparison with the structural features observed directly. The model serves to show strikingly the role of the size factor in determining film structures. In particular, it shows that for size differences near 25% amorphous structures are obtained over a wide range of compositions. It also shows that such amorphous structures are essentially unchanged by vibration "annealing." On the periodically grooved substrate, the existence of an "epitaxial" deposition rate is demonstrated. These and other features of the model are compared with experience concerning evaporated thin films and found to be in excellent qualitative agreement.

1. Introduction

Recent work in this laboratory¹⁻³ has shown that metastable solid solutions can be formed by the simultaneous evaporation of two metals onto a substrate maintained at a low temperature. The structure of the alloy thin films so obtained is amorphous in some cases and crystalline in others. In attempting to establish criteria for predicting when amorphous structures will be formed, as well as to understand the stability of such amorphous structures toward low-temperature anneals, we were led to consider a model for simulating such alloys. In this model, a single layer of hard spheres (plastic balls) of two different sizes is used to simulate the two types of atoms involved. The interatomic repulsive forces are thus automatically represented. To furnish an "attractive force," the spheres are introduced onto a tilted flat surface so that they roll together. Such forces represent only a very crude approximation to the actual forces among metal atoms. The model permits the study of the effects of a number of variables: composition, rate of "deposition," and size difference between the two types of spheres. The following additional features add to the versatility of the model: (a) A magnetic vibrator placed below the tray permits the simulation of low-temperature "annealing" subsequent to the deposition of the layer. (b) The preparation of a reduced photographic transparency of the model permits optical (Fraunhofer) diffraction patterns of the two-dimensional array of spheres to be obtained. (c) The preparation of a grooved surface onto which the balls can be introduced offers the possibility for simulating epitaxial growth.

This paper reviews some of the results obtained with the above model, and shows that the model is remarkably successful in predicting a number of features which are actually observed experimentally.

In passing, it should be mentioned that in the past there have been numerous examples of simple models (both two- and three-dimensional) to simulate the structure of crystals and liquids. Among the two-dimensional models are the soap bubble model of Bragg and Nye⁴ which has been useful in the study of crystal defects (such as dislocations, vacancies and grain boundaries), as well as Hilsch's model⁵ of magnets to represent thin films of ionic crystals. Hard spheres have been used to form a twodimensional model by Turnbull and Cormia⁶ and a three-dimensional model by Bernal et al., showing the transition from the liquid-like to the crystalline state. Finally, optical Fraunhofer diffraction from a twodimensional array was studied by Taylor et al.8 by piercing holes in cardboard to form a two-dimensional grating. Similar experiments were carried out by Hosemann and his coworkers.9 Although the present model has features in common with each of the above models, it appears to be sufficiently different both in the arrangement used and in the objectives attained that it is worth reporting on in some detail.

2. Experimental details

The spheres used in these experiments are acrylic plastic balls of different sizes and colors. They are rolled into a

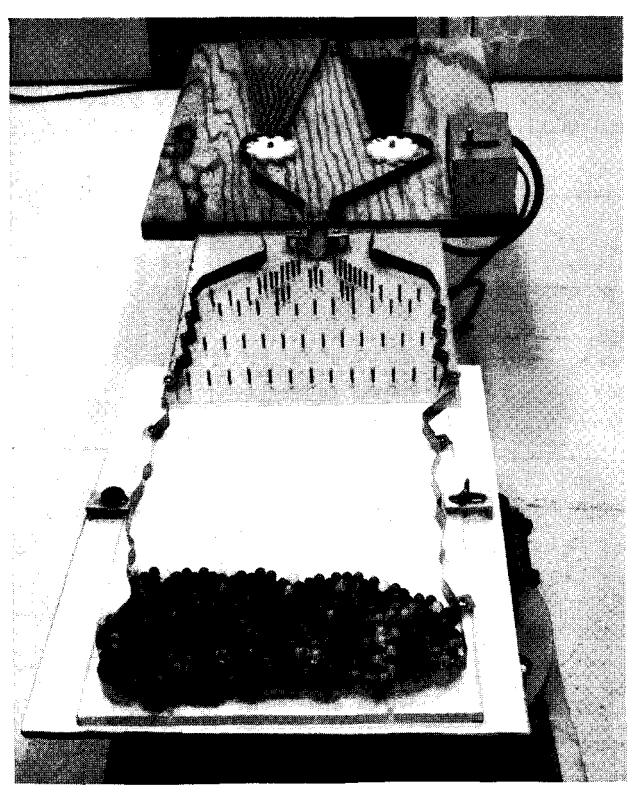


Figure 1 Equipment for producing a random mixture of spheres of two different sizes.

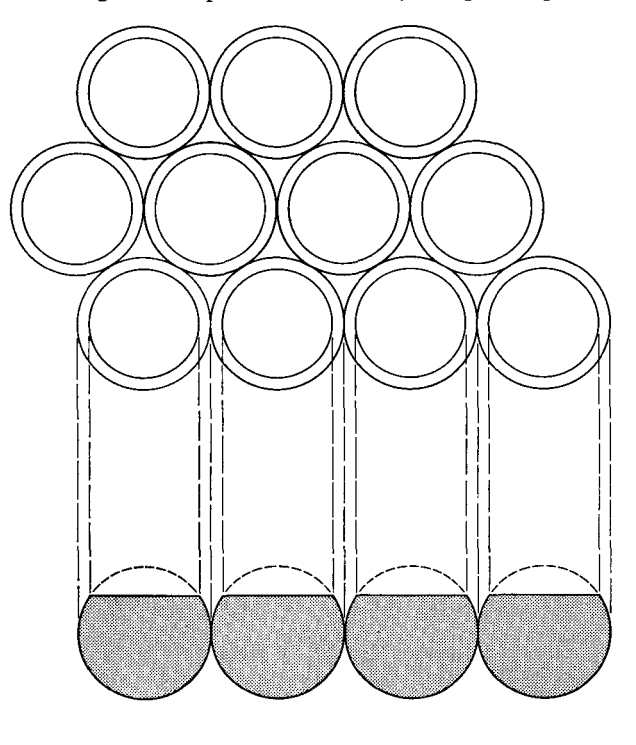
tray, normally tilted at an angle of 1.5° to the horizontal, by the device shown in Fig. 1. The top frame of the equipment contains reservoirs of balls of two different sizes. Below each reservoir is a slotted feed wheel which is motor driven at variable speeds chosen to control the rate of introduction of balls into the tray below. In each wheel, the sizes of the slots are made to match the size of the balls being introduced. The ratio of the numbers of spheres of the two sizes is controlled by varying the speed of rotation of the feed wheels, as well as by plugging up some of the slots in one wheel (if a very low concentration of one set of balls is desired). The pins in the second frame, below the one just described, serve to disperse the balls uniformly along the width of the tray. The bottom frame is the tray itself. The use of irregular corrugated walls on the tray is necessary in order to avoid the influence of the walls on the structure produced. For example, with straight walls and spheres all of one size, a regular close-packed structure is built up from each wall of the tray with a close-packed row parallel to the wall. When corrugated walls are used, this effect does not occur. The rate of introduction of the balls by the use of the feed wheels is such that the tray is filled in 5 to 10 min. This is designated as the "slow" rate. For relatively high rates of "deposition," balls were poured from a beaker directly above the pins, while still higher rates were achieved by pouring the balls over the second frame with the pins removed. These procedures fill the tray in 13 sec and 5 sec, respectively.

In the experiments on a "smooth substrate" (Section 3) the tray was a smooth, flat sheet of acrylic plastic (as shown in Fig. 1). In some experiments (Section 4) it was desired to simulate a crystalline substrate. For this purpose a grooved periodic layer was prepared as follows. First, a set of colorless balls (6.8 mm in diameter) was arranged into a perfect array and cemented to the substrate. Since the grooves thus produced are too deep to permit spheres to roll over them to form a second layer, the tops of the balls in this cemented layer were machined down as shown in Fig. 2. When the machining was carried to a depth of 1/16" and a tilt of the tray of 3.5° was used, the array of flat-topped balls simulated very well the effect of periodic potential due to the substrate, without eliminating the (gravitational) attractive potential which tends to pull together the balls introduced above this substrate.

A magnetic-type vibrator attached below the tray was used to simulate thermal annealing of the layer of balls subsequent to its deposition. The vibrator produced a side-to-side motion of the tray at sufficiently low amplitudes to avoid exciting balls to jump out of the layer. The standard vibration "anneal" was for a period of 5 min.

All experiments described here were carried out with

Figure 2 Preparation of a grooved periodic "substrate" by machining off the tops of a cemented layer of plastic spheres.



spheres of three diameters: 5.9, 6.8 and 7.8 mm. These are designated, respectively, as S, M and L for "small," "medium" and "large" throughout this paper. The spheres of each size were of a different color. Photographs of the arrays of spheres were taken as color transparencies. It was then possible to produce black and white reproductions with different degrees of contrast between the two sizes of spheres. Maximum contrast was sought when it was desired to use the model to show the location of "impurities" in the structure, while minimum contrast was required for the best results in the optical diffraction experiments,

To obtain diffraction patterns from the arrays, reduced negatives (with array size about 4 mm square) were prepared in which the balls appeared transparent on a dark background. The mean ball separation was then ~ 0.13 mm. Fraunhofer diffraction patterns were obtained from such a negative by passing light from a He-Ne laser ($\lambda = 6328$ Å) through a 3 mm diameter aperture placed in contact with the negative mounted on a 135 mm lens of a 35 mm camera. The photographs of the optical diffraction patterns shown in the present paper are enlargements of the pattern taken in this way, but using "dodging" methods to accentuate the outer rings of the pattern with respect to the inner details.

3. Arrays on a smooth substrate

• Spheres of one size

Since optical diffraction photographs will be used in the present work to evaluate the structure of an array of spheres, it is worthwhile to begin with the diffraction pattern from a perfect array. The array is presented in Fig. 3a while the corresponding diffraction pattern, obtained by the method described in the previous section, is shown in Fig. 3b. A hexagonal pattern of relatively sharp spots is obtained, reflecting the symmetry of the close packed array of spheres. These spots may be indexed in the manner of a diffraction pattern from a crystal, except that now only two indices are required. (See the Appendix).

An interesting modification is obtained by taking the diffraction pattern from an array consisting of two regions which have essentially the same orientation but are separated by a "stacking fault," as shown in Fig. 3c. The diffraction pattern, shown in Fig. 3d, is similar to that of a perfect array except for the appearance of streaks that run perpendicularly to the direction of the fault in the structure.

We are now ready to examine how a set of identical spheres arrange themselves when introduced by the method described in Section 2. Figure 4a shows the array obtained when the spheres are introduced at a slow rate,

through the use of the apparatus shown in Fig. 1, and Fig. 4b shows the corresponding diffraction pattern. The array of Fig. 4a was subsequently subjected to vibration at a constant amplitude for 5 minutes, during which time the spheres rearrange to the structure illustrated in Fig. 4c, giving the diffraction pattern of Fig. 4d. It is clear that this "annealed" structure consists of a small number of "grains" (regions of essentially perfect packing) of different orientations, and that the diffraction pattern is basically the superposition of two or three perfect-array patterns of the type already shown in Fig. 3b. (Note the stacking faults in the structure, as well as the "grain boundaries.") The as-deposited structure (Fig. 4a) has a larger number of grains than the annealed structure and therefore gives a larger number of superimposed perfectarray patterns, to the point where continuous rings begin to be produced (Fig. 4b). By contrast to the relatively slow deposition which produced Fig. 4a, a rapid rate of deposition was also used, where the entire layer was deposited in only a few seconds. Figure 4e shows that the grain size produced this way is much finer than for the slow deposition. The corresponding diffraction pattern (Fig. 4f) now shows definitely continuous rings (like the Debye-Scherrer rings in diffraction from crystals) with evidence of some preferred orientation, in that the intensity around the rings is nonuniform. The indexing of these diffraction rings is discussed in the Appendix. In summary, the rapid rate of deposition produces a more disordered (finer grained) structure than does the slow rate, while "annealing" produces considerable grain growth. Diffraction patterns are obtained which vary from a superposition of two or three "single crystal" patterns, for the "annealed" array, to one consisting of continuous rings characteristic of a fine grained structure.

In order to follow the process of grain growth during the vibration "anneal," pictures of an array of identical spheres were taken at shorter intervals of time, as shown in Fig. 5. The array was deposited using the slow rate of deposition, and then followed by 5, 15 and 30 second "anneals." Comparison of Figs. 5a and 5b shows that in 5 seconds there is appreciable improvement of grain perfection, some grain growth, and the elimination of some stacking faults. After 15 seconds there is further grain growth and migration of stacking faults. Finally after 30 seconds there is basically a two-grain structure separated by a stable high-angle grain boundary. Note that there are regions of this grain boundary where the two grains fit together rather well, and other regions of poor fit in which the density of spheres is relatively low. This picture compares rather well to the model of a high-angle grain boundary proposed by Mott.10 Similar structures of boundaries have also been seen in the soap-bubble model.4

It is also possible to observe a density change of the array during the process of vibration annealing. In Fig. 5a

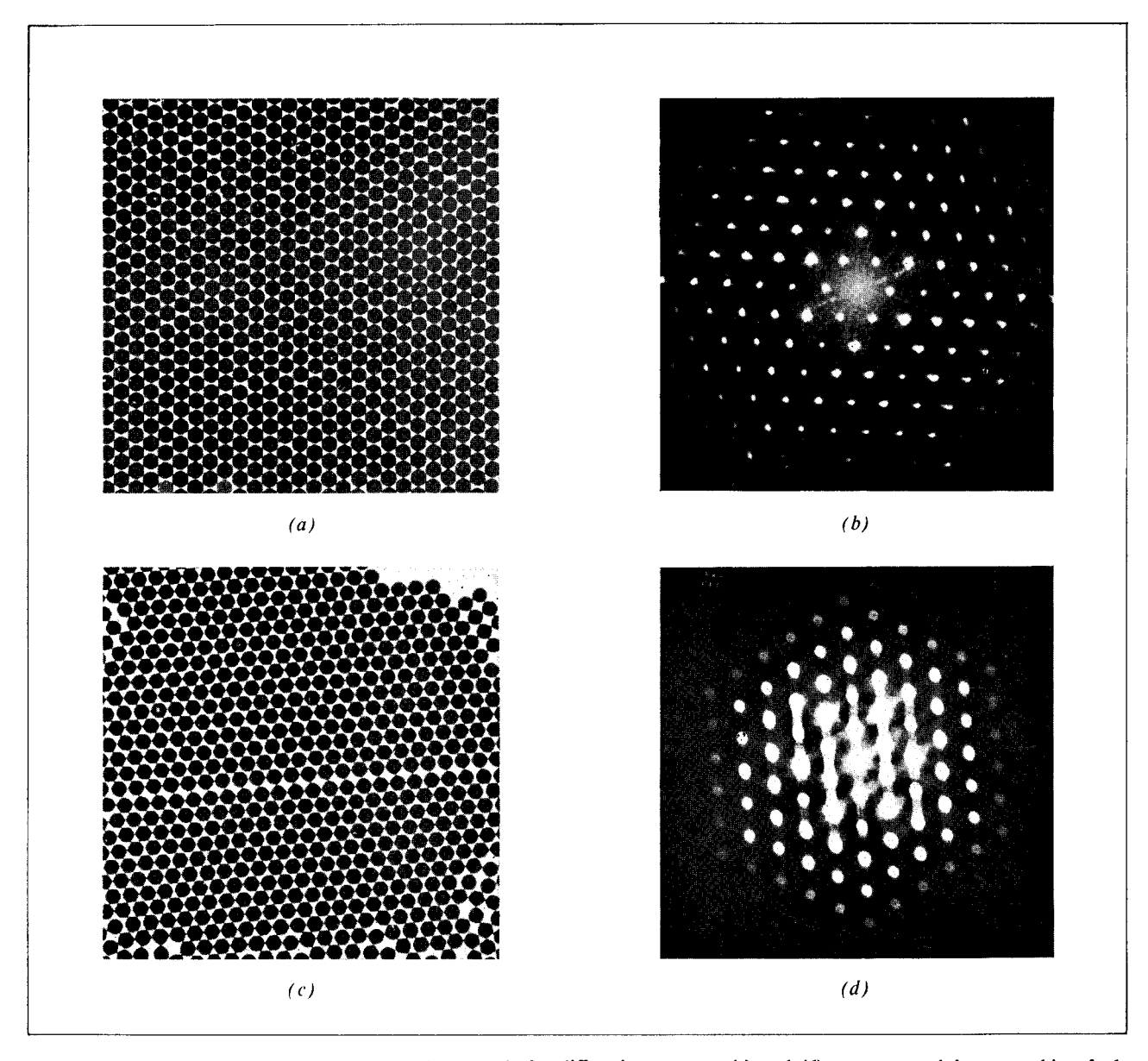
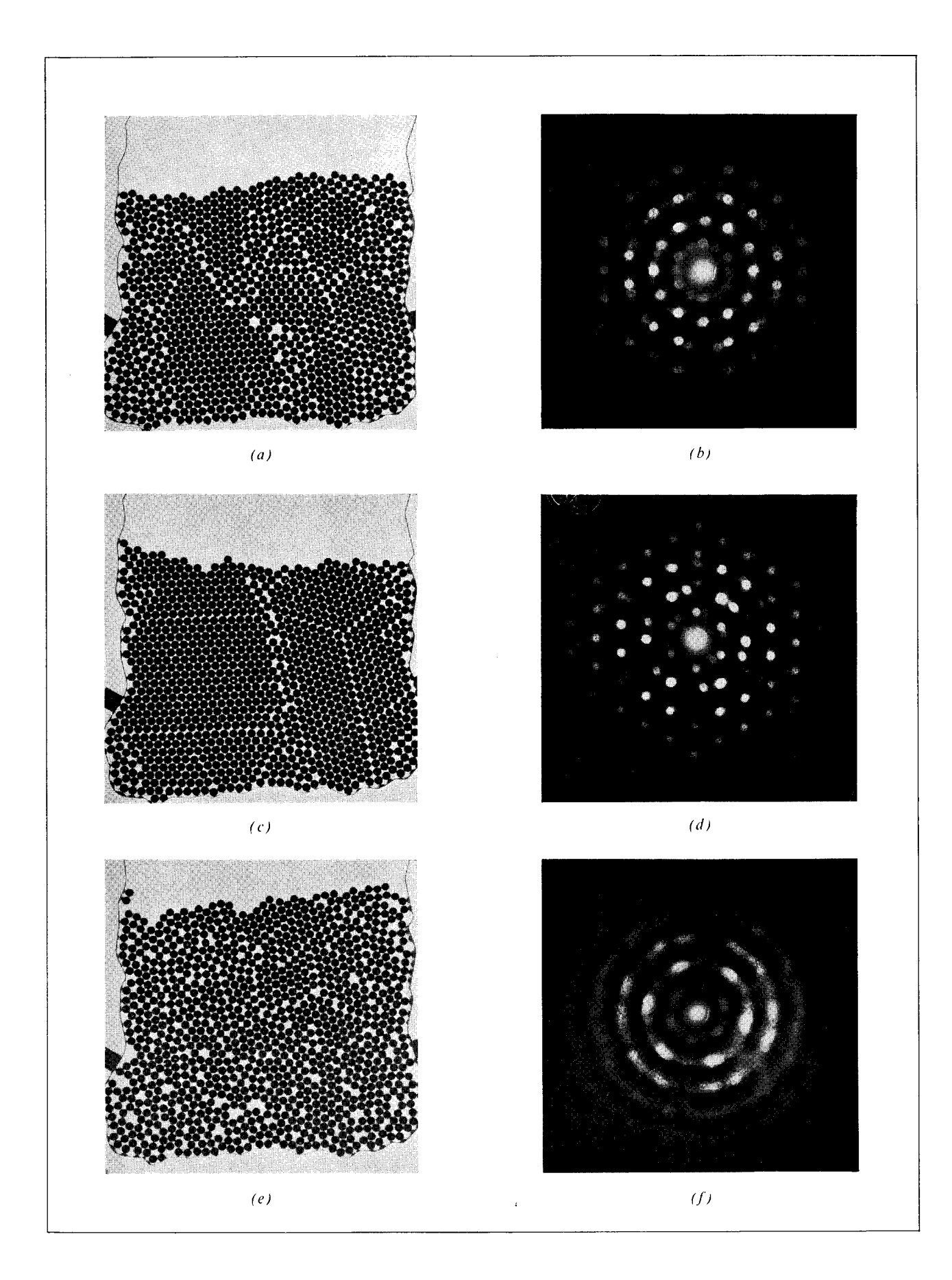


Figure 3 (a) Perfect array of spheres and (b) its Fraunhofer diffraction pattern; (c) and (d), array containing a stacking fault and its diffraction pattern.

an irregular line is drawn following the contour of the top of the array. The presence of this line allows a ready estimate of the increase in density which occurs as the structure is vibrated (Figs. 5b-d). This same method was also used to estimate the change in density upon annealing of the various "alloy" structures described below.

• Dilute "alloys"

We now turn to cases in which a small fraction of spheres of a different size from the major constituent (either smaller or larger) are introduced to form dilute "alloys." It is consistently found that for a given deposition rate, the grain size of the "alloy" in the as-deposited condition is smaller than for the case of identical spheres. The extent of the reduction in grain size depends on the size difference between the two types of spheres, as will be discussed below. The effect of a high rate of deposition is to reduce the grain size still further, in a manner analogous to the case of identical spheres (compare Figs. 4a and 4e). "Annealing" by vibration again produces grain growth,

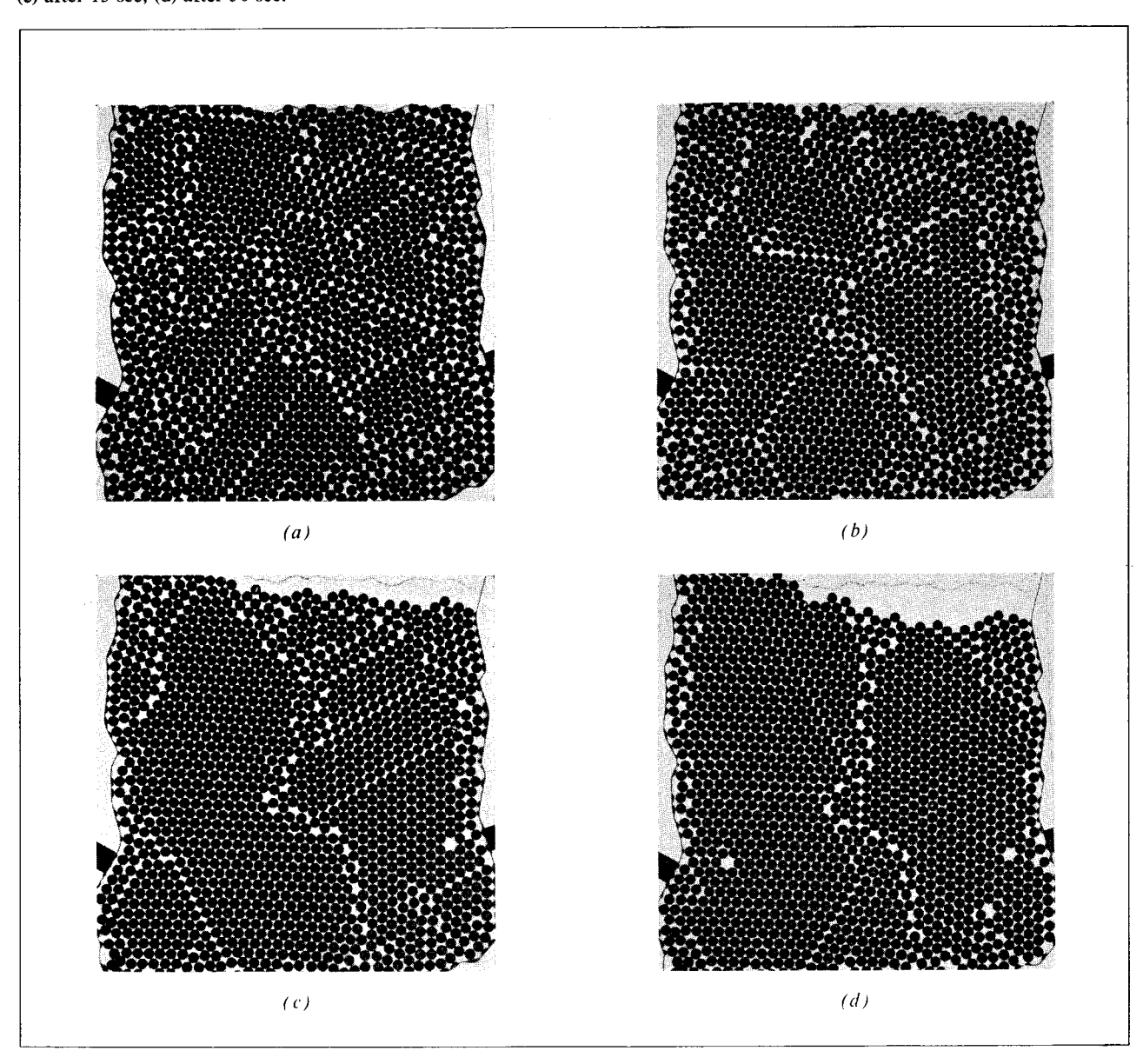


generally at a somewhat slower rate than that shown in Fig. 5 for the "pure" array. The final grain size after annealing is also smaller for the alloys than for the "pure" array. In Fig. 6, a set of examples are given of dilute alloys after vibration annealing. The four examples shown cover the cases of impurities which are both smaller and larger than the "solvent" spheres, as well as two different size factors. Recalling the terminology (see Section 2) that S,

M and L represent the small, medium and large size balls, we note that the alloys shown in Fig. 6 are, respectively, 95%S + 5%L, 90%S + 10%M, 95%L + 5%S, and 90%M + 10%S. Figures 6a and 6c show that for the L-S alloys (size difference $\sim 27\%$) of either the L-rich or S-rich types, the effect of the presence of only 5% of impurity spheres is to restrict grain growth substantially. Further, it is noteworthy that in these two cases there is

Figure 4 Results on spheres all of the same size. (a) and (b) Array produced at slow rate of deposition and its diffraction pattern; (c) and (d) array shown in (a) subjected to vibration "anneal;" (e) and (f) array produced at a high rate of deposition. (See page 362.)

Figure 5 Steps in the vibration "annealing" of an array deposited at a slow rate. (a) As deposited; (b) after 5 sec of vibration; (c) after 15 sec; (d) after 30 sec.



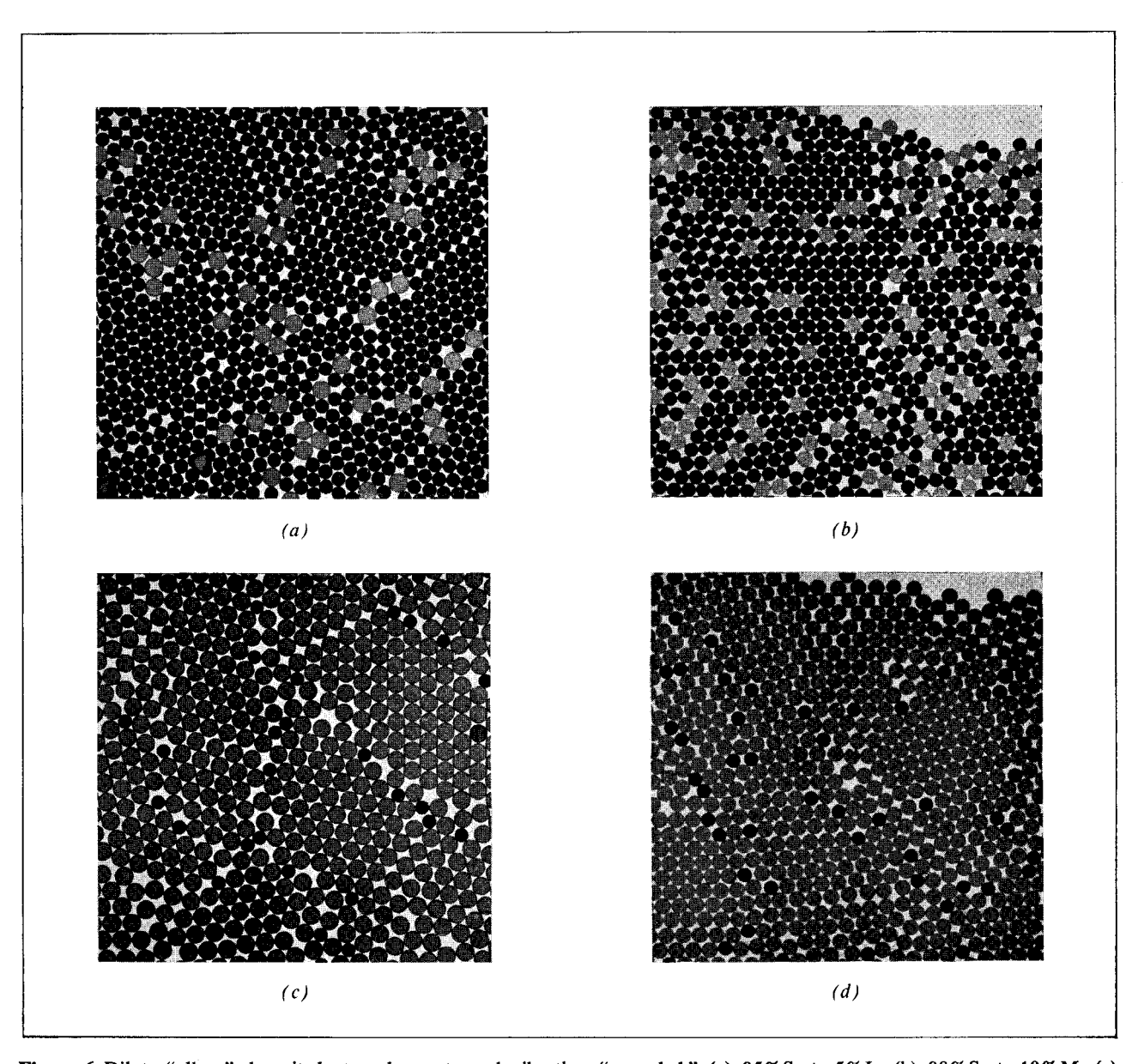


Figure 6 Dilute "alloys" deposited at a slow rate and vibration "annealed." (a) 95%S + 5%L, (b) 90%S + 10%M, (c) 95%L + 5%S; (d) 90%M + 10%S (where S, M, L represent the small medium and large sizes of spheres, respectively).

a strong tendency for the impurities to be located at the grain boundaries, leaving grains relatively free of impurities. On the other hand, Figs. 6b and 6d show that, for the S-M alloys (size difference $\sim 14\%$), even 10% of impurities are readily incorporated into the grain structure. Thus, the grain sizes of the S-M alloys are larger than those of the S-L alloys, although there is distortion (or "strain") within the grains of the former due to the incorporation of the impurities. This distortion may be seen as a bending of the rows of atoms in Figs. 6b and

6d, but without the formation of high-angle grain boundaries of the type discussed above.

• Concentrated "alloys"

The structure of arrays of spheres of various compositions, both in the as-deposited and "annealed" states, were examined for "alloys" of the S-M and S-L "systems." In all cases the slow deposition method (i.e., involving the feed wheels) was used. The grain size in the as-deposited condition continues to decrease as the concen-

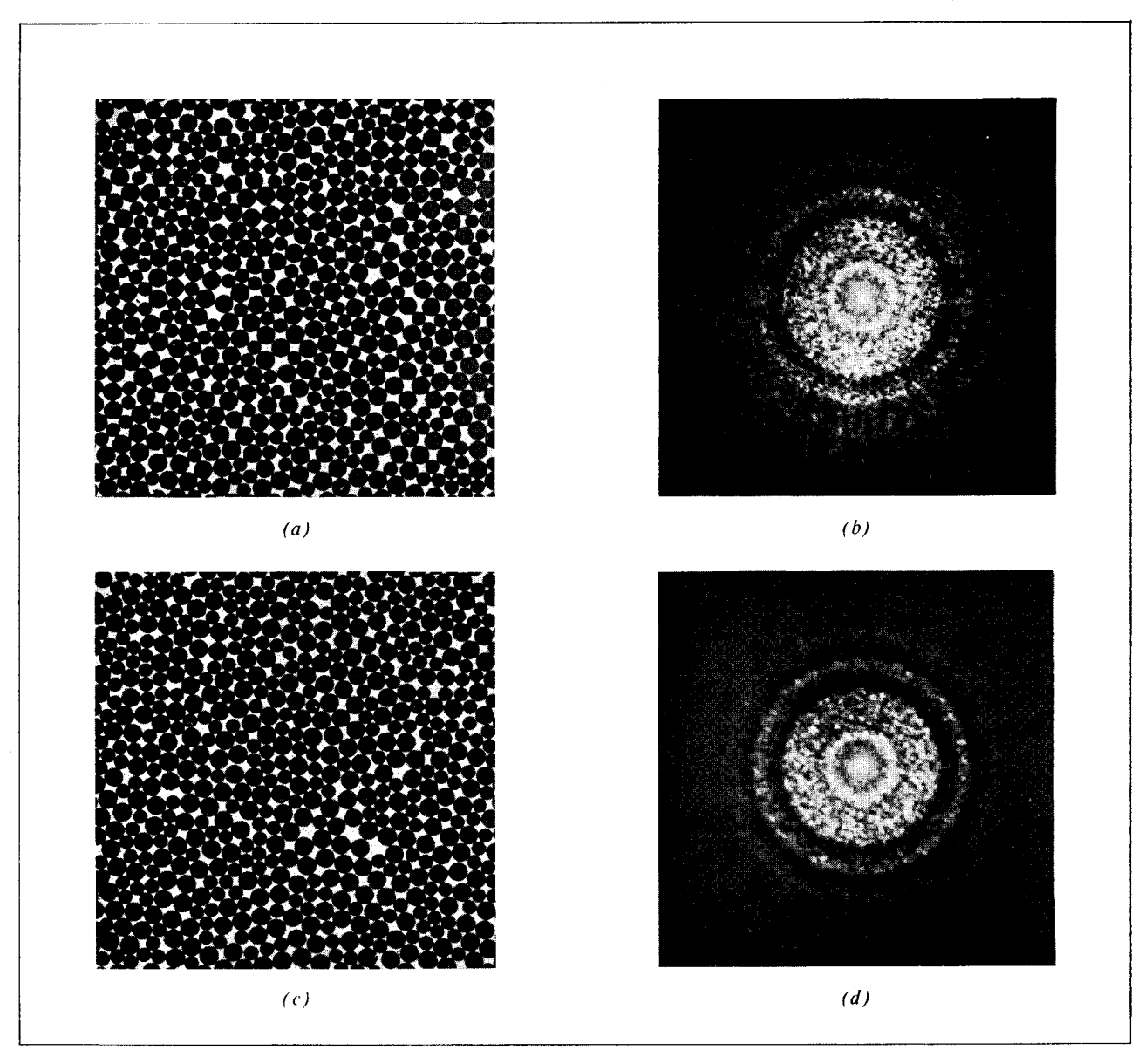


Figure 7 Alloy of 50%S + 50%L showing the amorphous structure: (a) and (b) as deposited; (c) and (d) after vibration "anneal."

tration increases. For the S-L system, at compositions between 40% and 60%L, a structure is obtained which can only be described as "amorphous," since one cannot identify a grain structure in it even on a scale of 2 to 3 sphere diameters. This structure is shown in Fig. 7a for the 50% alloy. The corresponding diffraction pattern (Fig. 7b) shows the disappearance of the second and third diffraction rings, which become part of a broad background of intensity. Vibration annealing of this structure produces an increase in the density of packing of the

spheres by about 5%. There is, however, no significant change either in its structure or in its diffraction pattern (Figs. 7c and 7d). One can ascribe the failure of vibration to produce grain growth to the formation of a type of "log jam" among these spheres of two substantially different sizes.

The 50% alloy shown in Fig. 7 may be contrasted to the case of the 17%S + 83%L alloy, shown in Fig. 8, which typifies the high concentration alloy whose structure may be designated as "crystalline." Here, all diffrac-

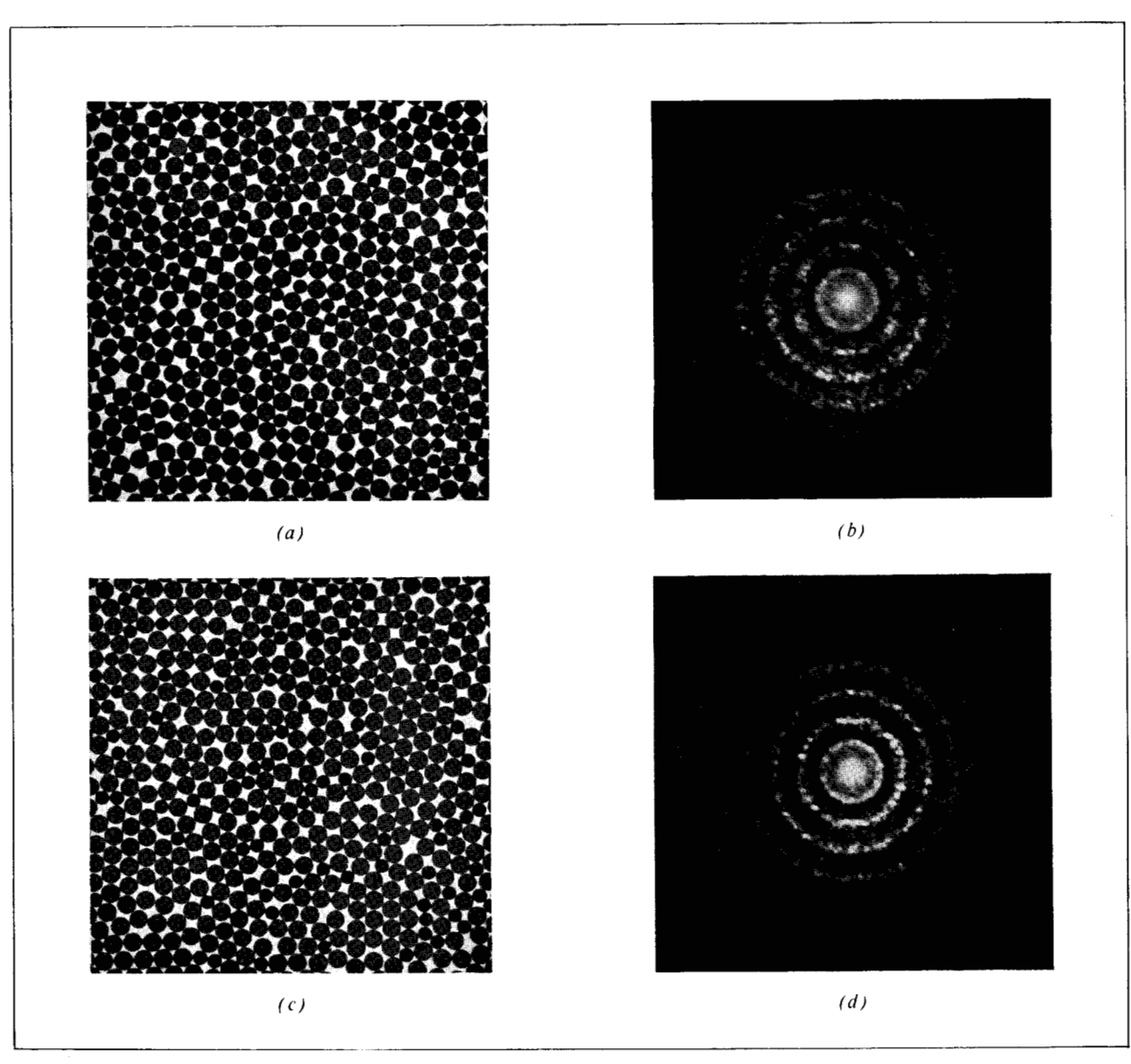


Figure 8 Alloy 17% S + 83% L showing crystalline structures: (a) and (b) as deposited; (c) and (d) after vibration "anneal."

tion rings are present in the as-deposited state, although they are broad because of the extremely fine grain structure. Vibration annealing (Figs. 8c and d) produces definite grain growth and a sharpening of the diffraction rings. The change in the density of packing of the spheres is also about 5% in this case. In fact, it is interesting to note that in all structures, including the "pure" array, a change in density upon annealing of close to 5% is observed. The "pure" spheres or dilute alloys deposit in a higher density than do the concentrated alloys, but the *increase* in density after vibration annealing is completed

turns out to be very nearly the same in all cases. In order to summarize the results for the various alloy arrays in as effective a manner as possible, we may develop a pseudo "phase diagram" showing the structures for the as-deposited and annealed cases for various compositions. Such a diagram is given in Fig. 9 for the S-L alloys and in Fig. 10 for the S-M alloys. The darkened circles show structures which were clearly crystalline, with different sizes of circles to represent different grain sizes. The loss of a well-defined second diffraction ring (as in Fig. 7) was used as the criterion for

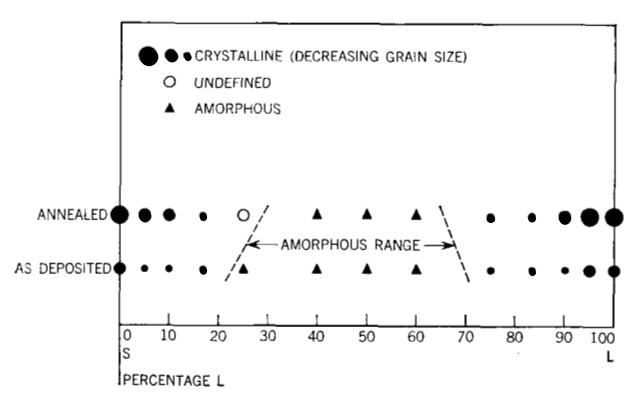
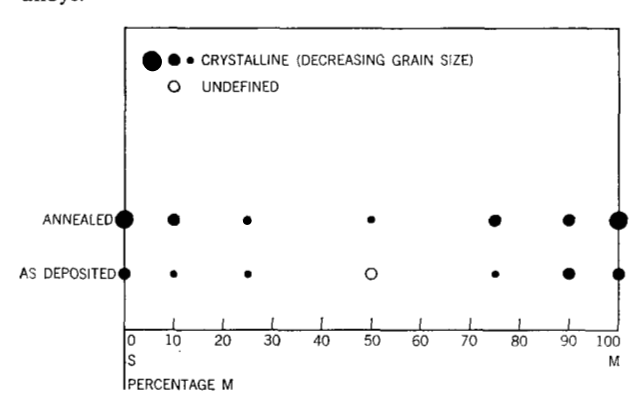


Figure 9 Pseudo "phase diagram" for S-L alloys, showing the region in which amorphous structure is obtained for both as-deposited and "annealed" conditions.

Figure 10 Diagram similar to Figure 9 for the case of S-M alloys.



designating a structure as "amorphous." The symbol X is used in Fig. 10 to designate the amorphous structure, while an open circle is used for a structure which is borderline between amorphous and crystalline (designated "undefined"). As already mentioned, in the middle region of the S-L diagram (size difference $\sim 27\%$) amorphous structures are obtained in both the as-deposited and annealed conditions. On the other hand, for the S-M diagram (size difference ~14%) there are no clearly amorphous structures. Another point of interest is the slight asymmetry of these two diagrams. For example, the amorphous range in the S-L diagram appears to extend more to the S-rich side than to the L-rich side. Also, in the S-M diagram, the grain size tends to be larger on the M-rich side. These results suggest that the larger impurities have a more disruptive influence on a lattice than do the smaller impurities.

4. Arrays on a "crystalline" substrate

In order to simulate a crystalline substrate, the grooved periodic structure (Fig. 2), prepared as described in Sec-

tion 2, was used. This substrate is made up from medium (M) sized spheres. Accordingly, we first investigated the structure obtained when spheres of this same size were deposited onto this substrate at various rates. Again, both the as-deposited and annealed structures were examined and Fraunhofer diffraction patterns were obtained. For the slow rate of deposition obtained using the feed wheels (Fig. 1), the array of Fig. 11a and diffraction pattern of Fig. 11b were obtained. This as-deposited structure is mainly a perfect alignment with the substrate, although there are some imperfect regions. (It will be helpful to note that in all of the photographs in the present section, the orientation is such that, for perfect matching to the substrate, the spheres must line up in vertical rows.) Upon annealing (Fig. 11c) the imperfect regions are mainly eliminated. The diffraction pattern (Fig. 11d) also shows the improvement in the structure. It is interesting to note that, since the imperfect regions in the as-deposited condition involve a lower density than that corresponding to perfect packing, the improvement of perfection during annealing must leave voids in the structure. Such voids are apparent in Fig. 11c.

Figure 12 shows a similar set of pictures for spheres introduced at a high rate (tray filled in 13 sec). The structure as deposited (Fig. 12a) is now much less perfect than that obtained with the slow rate of deposition, and its diffraction pattern (Fig. 12b) tends to show complete rings. Upon annealing (Figs. 12c and d), a much better alignment with the substrate is generally obtained, but a large grain of a different orientation is produced (see the lower right of Fig. 12c). The diffraction pattern, therefore, does not correspond simply to a perfect array. Deposition at a very high rate (tray filled in 5 sec) further enhances the deviation from alignment with the substrate and the tendency to form grains of different orientation upon annealing, as shown in Fig. 13. Here, the as-deposited structure is essentially random polycrystalline, while the annealed structure is still polycrystalline with some preferred orientation. These experiments then clearly show that slow rates of deposition favor "epitaxial growth" while high rates favor the loss of influence of the substrate.

Figures 11 to 13 show rather specifically how departures from epitaxy develop. It appears that whenever the local deviations from epitaxy are small in the as-deposited condition, vibration annealing always serves to bring these regions into better alignment with the substrate. However, if under high deposition rates a relatively large cluster of a different orientation is started, it continues to grow as more spheres are added. Further, such a cluster retains its different orientation upon annealing, although the degree of perfection of packing of the spheres increases. In this way a polycrystalline structure is formed.

In order to see what effect alloying may have on the question of epitaxial growth, we have carried out similar

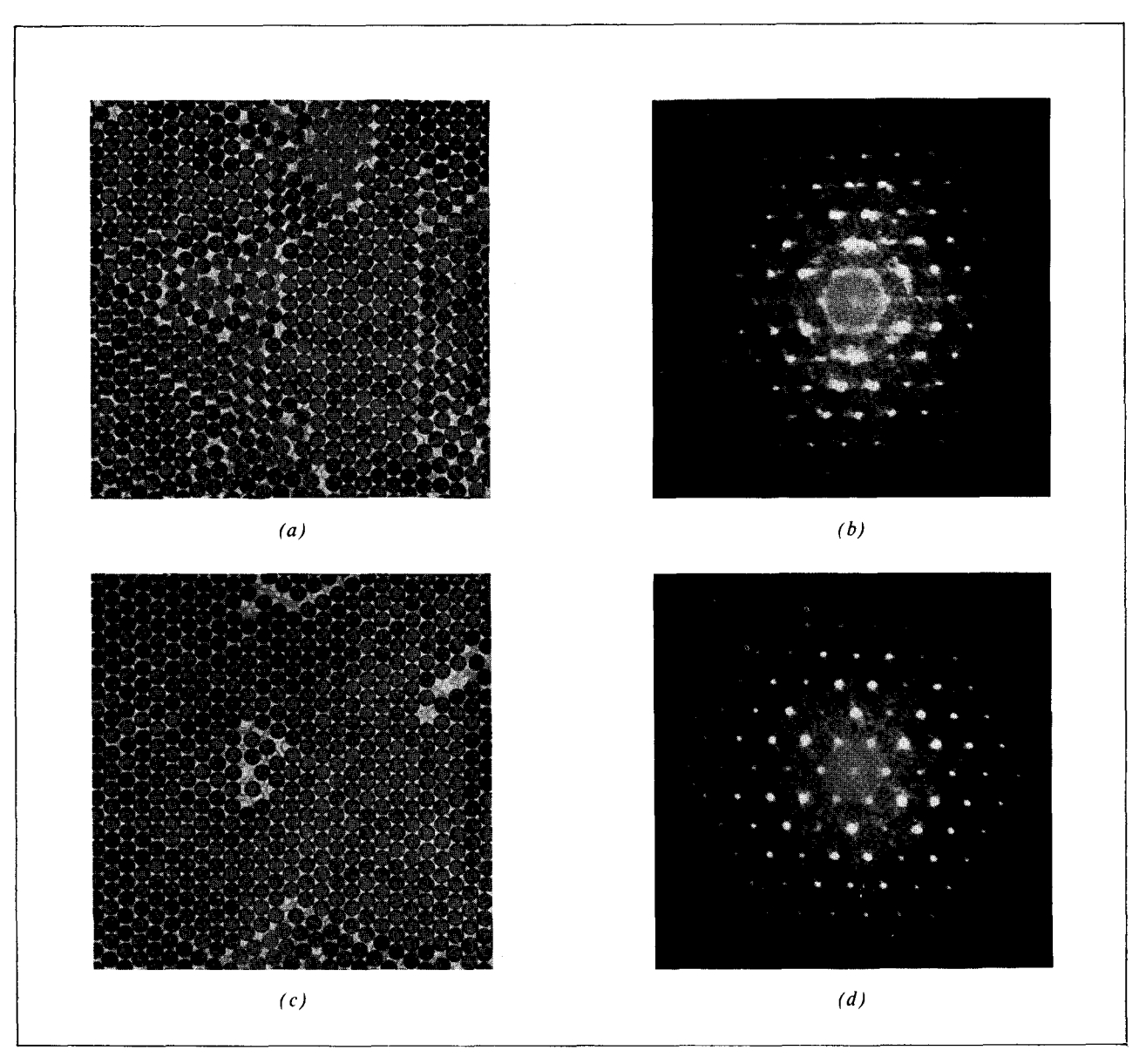


Figure 11 Arrays deposited at different rates on the grooved periodic substrate. Spheres all of same size (M) as the substrate periodicity; (a) and (b) as deposited at slow rate; (c) and (d) after vibration "anneal."

runs to the above for the case of the 90%M + 10%L alloy. Again at the slow rate (Fig. 14) we obtain a strong tendency toward alignment with the substrate in the asdeposited condition and with improvement upon annealing. There are, however, some regions of misalignment, and the diffraction pattern (Fig. 14d) is imperfect. The effect of the presence of 10% of larger spheres therefore is to impede somewhat the alignment with the substrate. For the high rate, analogous to Fig. 12, we now obtain the results shown in Fig. 15. This time the as-deposited structure may be described as random polycrystalline, and it

remains polycrystalline even after annealing, although some preferred orientation is evident. In fact, Fig. 15 closely resembles Fig. 13 for the case of pure spheres, although the array of Fig. 13 was obtained at a higher rate.

It is concluded that high rates of deposition give rise to relatively large regions with orientations different from the substrate. Such regions are relatively stable toward annealing and thus contribute toward polycrystalline rather than epitaxial structure. The presence of impurities serves to lower the "epitaxial rate," i.e., the deposition rate above which epitaxial growth is no longer obtained.

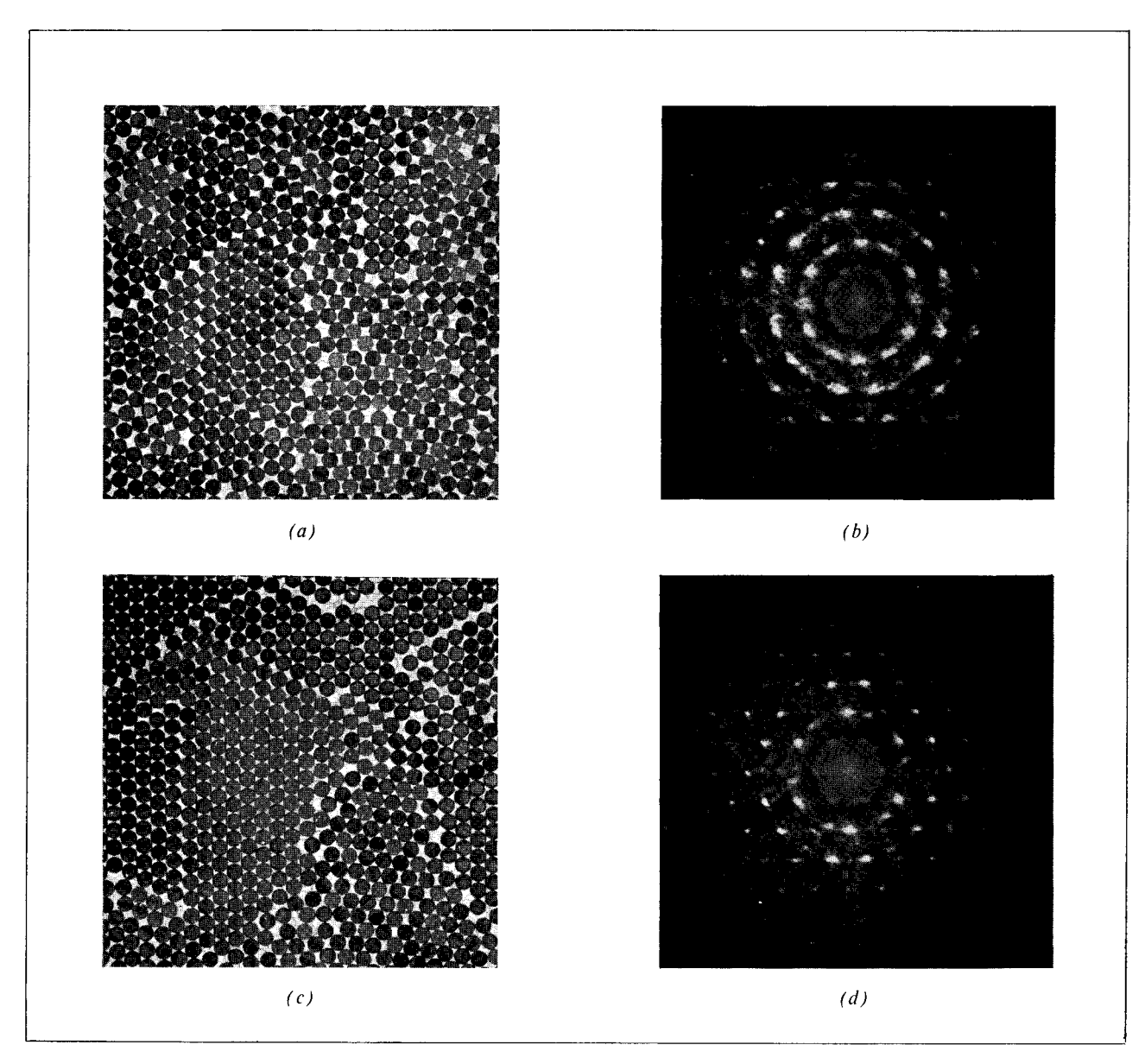


Figure 12 Same as Fig. 11 except for deposition at a high rate (13 sec).

5. Summary and comparison with experience

In this section we will compare the predictions of the present model against the corresponding experimental facts, whenever information is available from work on metal and alloy thin films. In this way, the usefulness of the model in making realistic predictions may be assessed. We begin with a summary of the principal conclusions which can be drawn from the model, as follows:

- 1. The higher the rate of deposition, the smaller the grain size obtained.
 - 2. A set of spheres which are identical in size always give a

"crystalline" structure, even for very rapid deposition rates. Vibration "annealing" then produces considerable grain growth and elimination of imperfections within the grains.

- 3. Dilute "alloys" show a finer grain size in the as-deposited state than do the spheres of only one size. Furthermore, "annealing" upon vibration is slower and less extensive for the case of alloys.
- 4. The effectiveness of impurities in impeding grain growth is determined by the difference in size between the impurity and the "solvent" spheres. In particular, it is observed that impurities which differ by $\sim 27\%$ in size from the solvent spheres are segregated heavily in the grain boundaries, while impurities differing by $\sim 14\%$ in size tend to be incorporated into the grains.

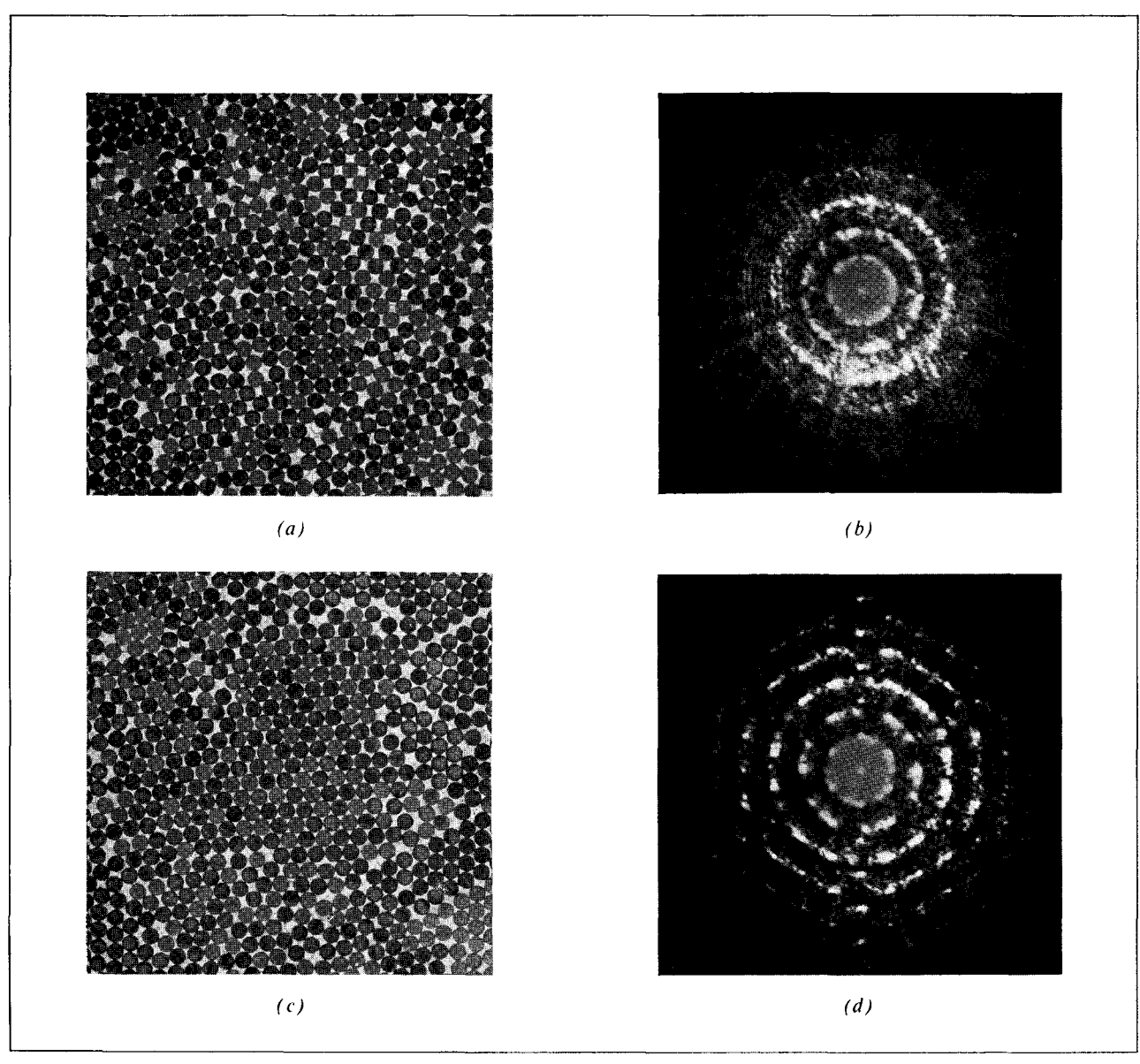


Figure 13 Same as Fig. 11 except for deposition at a very high rate (5 sec).

- 5. For concentrated "alloys" composed of two sets of spheres differing in size by \sim 27%, amorphous structures are obtained in the composition range of about 30–70%. Amorphous structures are not obtained at any compositions for alloys composed of spheres differing in size by \sim 14%.
- 6. One cannot draw a clear line between structures that would be classed as crystalline and those regarded as amorphous. There is, in fact, a continuous range of structures observed, spanning the gap between the clearly crystalline and clearly amorphous cases.
- 7. When an amorphous structure is deposited, it generally remains amorphous after vibration "annealing," although an increase in density occurs. This is a consequence of the fact that the "log-jam" in the structure cannot be relieved by vibration.
- 8. The tendency to form an amorphous structure is slightly greater for alloy compositions richer in small spheres than for

- those richer in large spheres. Also, for crystalline alloys, the grain size tends to be smaller on the small-rich side than on the large-rich side.
- 9. The structure obtained on a "crystalline" substrate depends on the rate of deposition. For rates below some critical value (the "epitaxial rate") one obtains essentially an epitaxial structure, whose perfection improves on annealing. Above this rate, one obtains a polycrystalline structure which becomes better defined, but remains polycrystalline, upon annealing. The epitaxial rate is not sharply defined. Rather, as the rate lessens the perfection continues to improve.
- 10. The presence of impurities which differ in size from the substrate periodicity lowers the epitaxial rate.
- 11. Improvement with annealing in the perfection of an epitaxial structure results in the development of voids to compensate for the local increase in density of the spheres.

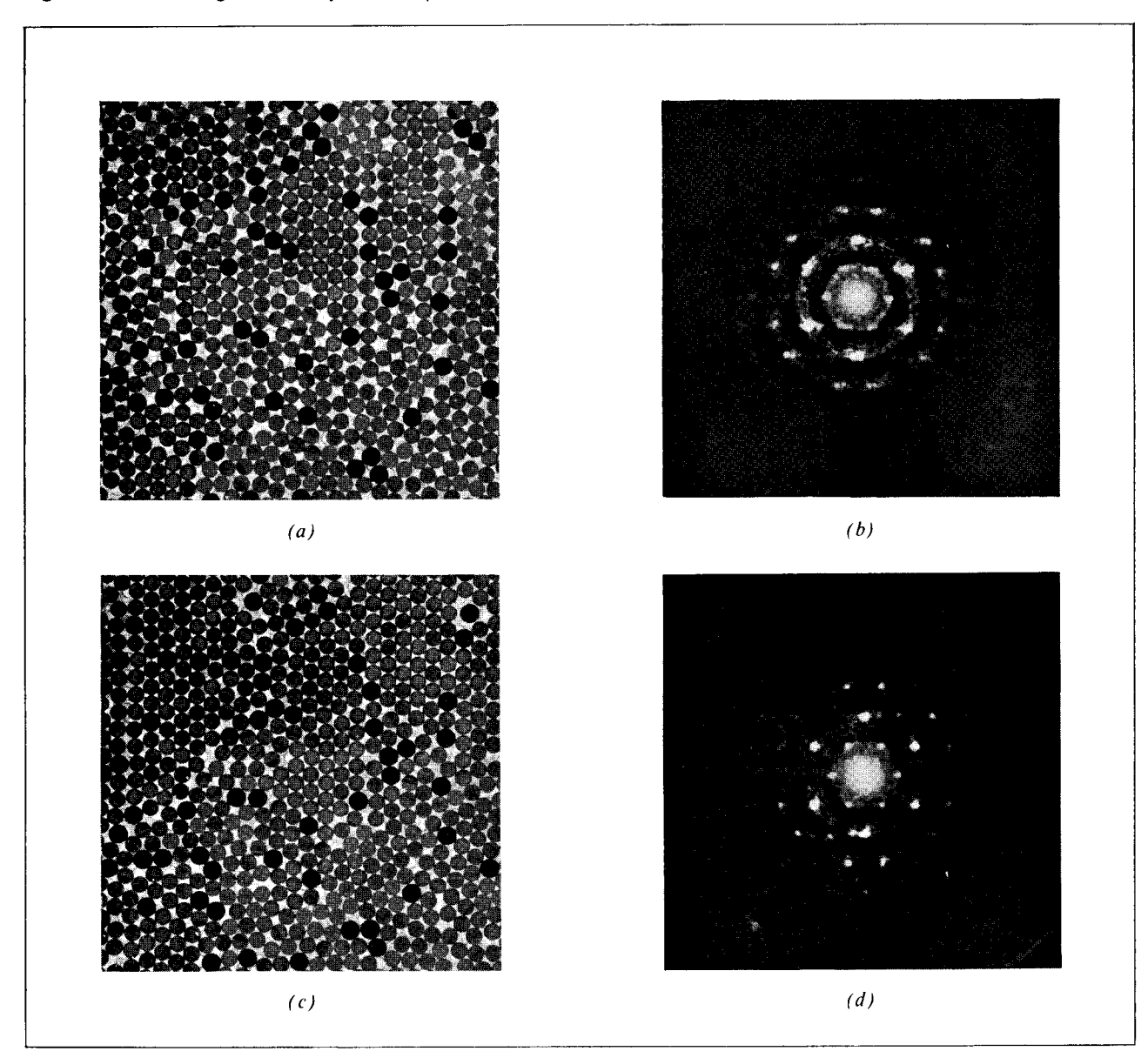
It should also be realized that the vibration anneal carried out with the present model simulates only low temperature annealing, i.e., corresponding to relatively long phonon wavelengths. Annealing processes which occur with activation energies corresponding to diffusional jumps are clearly not simulated by the model, since mechanical vibration does not provide the highly localized fluctuations in energy that make such jumps possible.

In order to check the above predictions against experience, we require, in general, experiments on films deposited at low temperatures. In this way the arriving atoms can stick essentially where they hit the substrate, with no

opportunity to undergo appreciable migration along the surface, similarly to the situation in the model. Such low-temperature depositions have been carried out mainly by Hilsch and his school¹¹ and by the present authors.^{2,3} In what follows, we will review the above predictions one by one, citing appropriate experimental work where available.

- 1. The fact that the grain size decreases with increasing rate of deposition is well known. 12
- 2. Typical pure metals (e.g., Cu, Au, Al, Pb and Sn, for which bonding is metallic rather than covalent) show crystalline structures even when deposited at 4°K.¹³ With low-temperature annealing, these metals show rapid grain growth and improvement of perfection, as indicated by the sharpening of diffraction

Figure 14 Same as Fig. 11 for alloy 90% M + 10% L and slow rate.



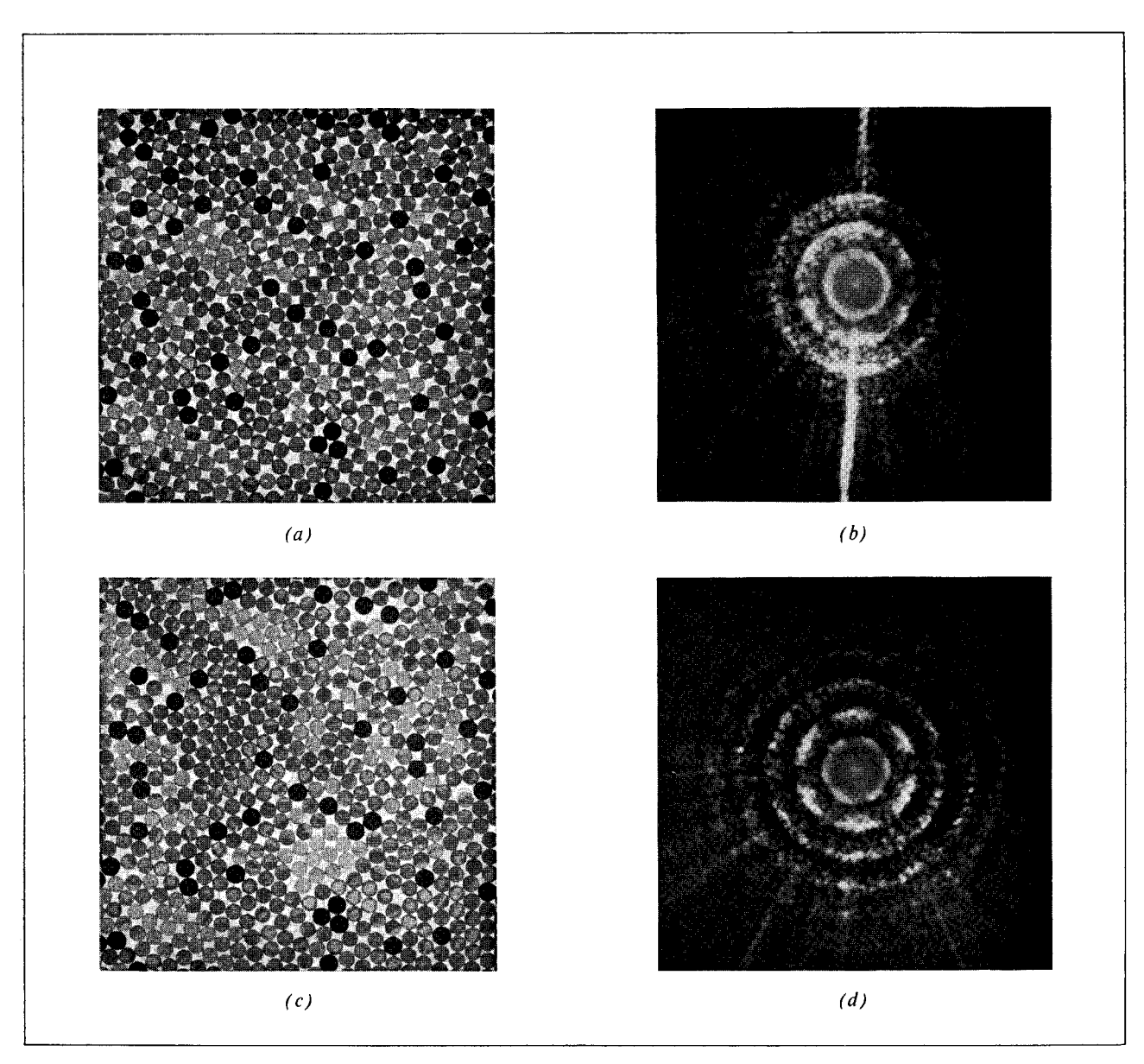


Figure 15 Same as Fig. 14 but at a high rate (13 sec).

lines, 14 the decrease in electrical resistivity, 15,16 and the release of stored energy, 17

- 3. The effect of impurities on the grain size of thin films, both as-deposited and after annealing, has been studied by Rühl¹⁸ for the case of gaseous impurities. In particular, Rühl finds a much smaller grain size in Sn films, both after deposition at 20°K and after heating to room temperature, for films deposited in a poor vacuum as compared to those deposited in a relatively high vacuum.
- 4. Evidence that impurities segregate at grain boundaries, the more so the greater the size difference between the solute and solvent atoms, has been given for bulk alloys through the use of internal friction techniques.¹⁹ It seems reasonable to expect similar results for thin film alloys, though direct evidence does not exist.
- 5. Recent work in this laboratory^{2,3,20} has shown that amorphous alloys can be produced by simultaneous deposition

of the two components onto a cold substrate. Amorphous structures are obtained over a wide range of compositions for the alloys Cu-Mg, Co-Ag and Co-Au, all of which have size differences greater than 15%, and over a narrower range (35 to 65%) for Ag-Cu alloys (size difference of 12%). No amorphous structures are obtained, however, for Co-Cu alloys (size factor 2%). These results are in qualitative agreement with the predictions of the model.

- 6. When an amorphous alloy is heated with a gradual increase in temperature, the diffraction pattern is observed to change continuously from one showing two broad halos to a pattern which is definitely crystalline. Further, different amorphous alloys show differing amounts of detail in their diffraction patterns. For the morphous alloys show differing amounts of detail in their diffraction patterns.
- 7. It has been observed^{2,3} that the amorphous structure, once formed, is stable to relatively high temperatures (generally above room temperature for alloys involving higher melting

metals such as Cu, Au, Co). Furthermore, the transformation from amorphous to crystalline involves a relatively high activation energy (\sim 1 eV), which is suggestive of some sort of diffusion jump. As already mentioned above, the vibration "annealing" of the present model simulates only low-temperature annealing effects, not annealing which gives rise to diffusion. The fact that crystallization is not observed in the model therefore provides a basis for understanding of the relatively high stability of the amorphous phase.

8. The amorphous range in the Co-Au alloys is observed 20 to go from about 20 to 65 atomic % Au. It is noteworthy that in this case the amorphous range extends further on the small-atom rich side than on the large-atom rich side of the phase diagram.

- 9. The existence of an "epitaxial temperature," below which a polycrystalline and above which a single-crystalline structure is obtained, is well known. It is also well known that the rate can be varied instead of the temperature, since the important quantity is the degree of supersaturation. The work of Sloope and Tiller, a where both rate and temperature are varied, illustrates this point for Ag deposited on rock salt. It is also well known that the epitaxial temperature or epitaxial rate is not a sharp dividing line, i.e., that perfection of a deposit continues to increase with increasing temperature or decreasing deposition rate.
- 10. There is no unambiguous evidence on the effect of impurities on epitaxy. Gaseous impurities, due to imperfect vacuum, are known to raise the epitaxial temperature, but unfortunately the state of surface cleanliness is then also changed.
- 11. Several workers²²⁻²⁴ have observed oriented polyhedral holes in epitaxial thin films, which may be formed by a mechanism similar to the void formation in the present model.

In summary, it is striking to find that there is experimental evidence in support of most of the predictions made by the present model. We may conclude, therefore, that the model serves to simulate the qualitative aspects of the structure of metal and alloy thin films to a better degree than might have been anticipated.

Acknowledgments

The authors are indebted to K. W. Asai, who designed the equipment shown in Fig. 1 and carried out most of the experiments on the preparation of the various arrays. They also wish to thank Miss S. Clarke for her skillful work on the optical diffraction photographs.

Appendix: Discussion of diffraction patterns

The first contribution to the diffraction pattern which must be considered is that of a single circular aperture. Clearly, if the array consisted of a random and widely spaced collection of N spheres, all of the same size, the total diffraction obtained would be N times that for a single circular aperture. It is well known²⁵ that such an aperture gives a series of maxima and minima in intensity at diffraction angles which may be described by

$$\sin \theta = p\lambda/a, \tag{A.1}$$

where θ is the angle between the incident and diffracted beams, λ the wavelength, a the aperture diameter, and p is (in general) an irrational number which for the first

few maxima takes on values 0, 1.64, 2.67, 3.69, 4.72 and for the minima the values 1.22, 2.23, 3.24, 4.24, 5.24 (all values rounded off to three figures). In the present optical patterns, because of the touching of the spheres and tendencies toward local ordering, none of the diffraction patterns observed are directly describable in terms of the single-aperture diffraction. Rather, the single-aperture factor serves to modulate the intensities of the sharper maxima which are obtained as a result of interference effects between the individual apertures.

The diffraction by a perfect array of spheres (which is an array of circles on the photograph from which the diffraction pattern is obtained) obeys the relation

$$n\lambda = d\sin\theta, \tag{A.2}$$

where n is the (integral) order of the diffraction maximum and d the spacing between a parallel set of lines through the centers of the spheres. For the perfect hexagonal array this becomes

$$\sin \theta = (2n/\sqrt{3})(h^2 + hk + k^2)^{\frac{1}{2}}\lambda/a,$$
 (A.3)

where (hk) is the two-index specification of a set of parallel lines in the two-dimensional array, analogous to the Miller indices of a set of planes in a crystal.

When the grain size becomes fine enough, continuous Debye-Scherrer type rings are obtained. The higher order diffractions then tend to be weak, so that the four strongest diffractions observed (starting from the innermost ring) are, respectively, to (hk) = (10), (11), (21) and (31), all with n = 1.

Finally, the inner part of the amorphous pattern is also due to interferences, i.e., to correlations among the positions of the spheres. This statement is based on the fact that it is not possible to describe this pattern solely as the superposition of the patterns due to single circular apertures of the two different sphere diameters.

References and footnotes

- E. Kneller, "Magnetic Moment of Co-Cu Solid Solutions with 40 to 85% Cu," J. Appl. Phys. 33, 1355 (1962); also ibid. 35, 2210 (1964).
- S. Mader, H. Widmer, F. M. d'Heurle and A. S. Nowick, "Metastable Alloys of Cu-Co and Cu-Ag Thin Films Deposited in Vacuum," Appl. Phys. Lett. 3, 201 (1963).
- S. Mader, "Metastable Alloy Films," J. Vac. Sci. Tech. 2, 35 (1965).
- W. L. Bragg and J. F. Nye, "A Dynamical Model of a Crystal Structure," Proc. Roy. Soc. A190, 474 (1947).
- R. Hilsch, "Ein Kristallgittermodell," Zeits. Physik 138, 432 (1954).
- D. Turnbull and R. L. Cormia, "A Dynamic Hard Sphere Model," J. Appl. Phys. 31, 674 (1960).
- J. D. Bernal, K. R. Knight and I. Cherry, "Growth of Crystals from Random Close Packing," *Nature* 202, 852 (1964).
- 8. C. A. Taylor, R. M. Hinde and H. Lipson, "Optical Methods in X-Ray Analysis. I. The Study of Imperfect Structures," *Acta Cryst.* 4, 261 (1951).

- See references in the book: R. Hosemann and S. N. Bagchi, Direct Analysis of Diffraction by Matter, North Holland Publishing Co., Amsterdam, 1962.
- 10. N. F. Mott, "Slip at Grain Boundaries and Grain Growth in Metals," *Proc. Phys. Soc.* (London) 60, 391 (1948).
- See, for example, the summary given by R. Hilsch in the book: Non-Crystalline Solids, Ed., V. D. Fréchette. John Wiley and Sons, Inc., New York, 1960.
- See, for example, R. E. Thun, "Structure of Thin Films" in *Physics of Thin Films I*, Ed., G. Hass, Academic Press, N. Y., 1963.
- 13. W. Buckel, "Some Remarks on Crystal Growth in Thin Films," in *Structure and Properties of Thin Films*, Ed. C. A. Neugebauer, J. B. Newkirk, D. A. Vermilyea, John Wiley and Sons, Inc., New York, 1959, p. 53.
- and Sons, Inc., New York, 1959, p. 53.

 14. H. Bülow and W. Buckel, "Elektronbeugungsaufnahmen von dünnen Metallschichten bei tiefen Temperaturen,"

 Zeits. Phys. 145, 141 (1956).
- Zeits. Phys. 145, 141 (1956).
 15. W. Buckel and R. Hilsch, "Einfluss der Kondensation bei tiefen Temperaturen auf den electrischen Widerstand und die Supraleitung für verschiedene Metalle," Zeits. Phys. 138, 109 (1954).
- E. Feldkeller, "Struktur und Widerstand sehr stark gestörter Kuperschichten bei tiefen Temperaturen," Zeits. Phys. 157, 65 (1959).

- W. Mönch, "Messung der Fehlordungsenergie an abschreckend kondensierten Metallschichten bei tiefer Temperatur." Zeits. Phys. 164, 229 (1961).
- peratur," Zeits. Phys. 164, 229 (1961).

 18. W. Rühl, "Röntgenographische Unterschungen an kondensierten Zinnfilmen bei tiefen Temperaturen," Zeits. Phys. 138, 121 (1954).
- J. Winter and S. Weinig, "The Grain Boundary Adsorption of Solutes," Trans. Met. Soc. AIME 215, 74 (1959).
- 20. S. Mader and A. S. Nowick, to be published.
- B. W. Sloope and C. O. Tiller, "Formation Conditions and Structure of Thin Epitaxial Silver Films in Rocksalt," J. Appl. Phys. 32, 1331 (1961).
- J. Appl. Phys. 32, 1331 (1961).
 V. A. Phillips, "Polyhedral Holes in Evaporated AuCu Films," J. Appl. Phys. 31, 697 (1960).
- 23. R. W. Vook, "Oriented Polyhedral Voids in Single Crystal Thin Films," Bull. A.P.S. 6, 24 (1961).
- A. Yelon, E. W. Pugh and O. Voegeli, "Switching Properties of Single Crystal Ni-Fe Films," International Conference on Magnetism, Nottingham, England, 1964.
- 25. See any book on physical optics, for example: F. A. Jenkins and H. E. White, *Fundamentals of Physical Optics*, McGraw-Hill Book Co., New York, 1937, Chap. 5.

Received June 1, 1965